Homopolymer Solubilization and Nanoparticle Encapsulation in Diblock Copolymer Micelles

Michelle D. Lefebvre and Kenneth R. Shull*

Department of Materials Science and Engineering, Northwestern University, Evanston, Illinois 60208-3108

Received January 16, 2006; Revised Manuscript Received March 9, 2006

ABSTRACT: We use self-consistent mean-field theory to investigate a system of A homopolymer, AB copolymer, and C homopolymer, where there are attractive interactions between the B and C components. We calculate volume fraction profiles and chemical potentials of formation for unswollen micelles, swollen micelles, and flat interfaces using a theory that is generalized for multiple components and a general copolymer composition distribution. We find that swollen spherical AB copolymer micelles form in the A matrix with a preferred radius that controls the amount of C homopolymer solubilized in the center of the micelle and that they form at chemical potentials lower than the chemical potential of micelle formation in the absence of C homopolymer. The swollen spherical micelles are also preferred over a flat interface geometry because the copolymer changes the preferred interfacial radius of curvature. The calculations also show that nanoparticles can be encapsulated in the center of swollen micelles by introducing an attraction between the surface of the particle and the C homopolymer. These results indicate that a nanocomposite could be formed by utilizing attractive B−C interactions to encapsulate C homopolymer and nanoparticles in AB diblock copolymer micelles.

Introduction

Block copolymers of two incompatible repeat units are unique because while the two components would normally macroscopically segregate, the connectivity of the chains prevents it. Instead, the chains self-assemble to form microscopic domains of a characteristic shape and size that depend on the length of the chain, the interaction parameter χ, and the ratio of the amounts of the two components. Several techniques have been developed to control the formation of the domains so that they have long range order, and these ordered films have been widely used as patterned templates for a variety of applications.[1−6] One such application is the use of diblock copolymers as templates for organizing the spatial distribution of nanoparticles. Many theoretical and experimental studies have been conducted on these nanocomposites, on both the effect of the copolymers on the position of the nanoparticles and the effect of the nanoparticles on the conformation of the copolymers.[7−20] Balazs and co-workers have published numerous theoretical papers on diblock copolymer melts with filler particles that create highly ordered nanocomposites.[8−17] In an experimental study, Chiu et al. use poly(styrene-*b*-2-vinylpyridine) (PS−PVP) diblock copolymers to precisely arrange PS- and PVP-coated gold nanoparticles at specific locations within the diblock lamellae.[7]

In this work, we address a different type of block copolymer mediated nanocomposite where the nanoparticles do not necessarily interact directly with one of the copolymer blocks, but instead with a homopolymer that is preferentially solubilized in a diblock copolymer micelle. In a blend of incompatible homopolymers, it is known that the addition of a block copolymer at the interface will lower the interfacial tension,[21−25] which is particularly useful for blend compatibilization.[26−33] Introduction of hydrogen bonding or a similar favorable interaction between two of the components in the system causes an increase in the adsorption of copolymer at the interface and an accompanying decrease in the interfacial tension.[34−37] As copolymer accumulates at the interface and the interfacial tension is lowered to near zero, the preferred interfacial curvature changes, leading to the formation of a variety of possible morphologies, including micelles, swollen micelles, or a bicontinuous microemulsion.[23,38−42]

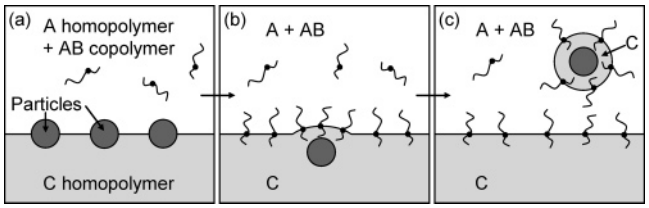

Figure 1. Formation of swollen micelle nanocomposites. (a) A layered sample is prepared by first depositing a layer of C homopolymer, then a layer of nanoparticles, and then a blend of A homopolymer and asymmetric AB copolymer. (b) Upon annealing, favorable interactions between B and C repeat units cause the copolymer to migrate to the A−C interface. Attraction between the particle and the C repeat units causes the particles to diffuse into the C phase. (c) When the interfacial tension is lowered by the copolymer, the interface develops curvature and micelles swollen with C form around the particles in the A phase.

We consider a system of phase-separated A and C homopolymers and an asymmetric AB diblock copolymer, where the B block is the shorter block and the B and C repeat units have favorable interactions, as shown in Figure 1. When the AB copolymer segregates to the A−C interface, the interfacial tension begins to decrease and the curvature begins to change. It is then possible to "pinch off" AB copolymer micelles with C homopolymer solubilized in the center, creating droplets of C homopolymer in the A homopolymer matrix that are stabilized by the AB copolymer and the favorable interactions between the C and B components. If, in addition, there is a layer of nanoparticles deposited at the interface between the homopolymers, the particles may also be emulsified in the swollen micelles and dispersed throughout the A homopolymer phase. This process can be enhanced by using a particle that has favorable interactions with the C homopolymer.

* Corresponding author: e-mail k-shull@northwestern.edu.

10.1021/ma060112w CCC: $33.50
Published on Web 04/05/2006

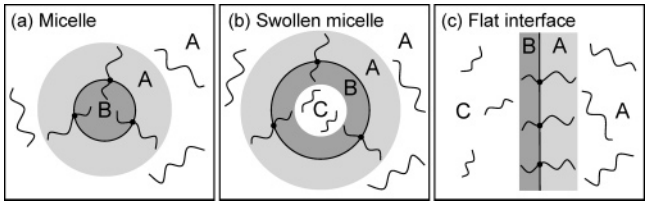

Figure 2. Copolymer interfacial radius of curvature: (a) micelle, $R \approx 2-3$ times R_{gc}; (b) swollen micelle, intermediate curvature; (c) flat interface, R approaches infinity.

An example of a hydrogen-bonding system that could be used to form these nanocomposites is one containing a polystyrene (PS) homopolymer, a poly(2-vinylpyridine) (PVP) homopolymer, and a block copolymer of PS and poly(4-hydroxystyrene) (PHS), where the hydroxyl group in the PHS and the nitrogen in the PVP can undergo hydrogen bonding.[23,36,37,39] This system differs slightly from some of the previous studies using these polymers in that the PVP is the droplet phase instead of a block of the copolymer. Using PVP as the droplet phase has the advantage that PVP interacts strongly with many inorganic materials. The addition of particles made from these materials at the PS/PVP interface could allow the formation of a nanocomposite where each individual particle is coated with a layer of PVP homopolymer and surrounded by copolymer, and the spacing between each particle can be controlled by the dimensions of the polymeric components.

The important parameter in this system is the radius of curvature of the interface that is modified by the copolymer molecules.[38] There are three possible configurations of the interface: a micelle, a swollen micelle, or a flat interface. Schematics of all three structures are shown in Figure 2. In an unswollen micelle, the shorter, incompatible B block forms the core, while the A block forms the corona that is miscible with the A matrix, as shown in Figure 2a. The micelle can have spherical, cylindrical, or lamellar geometry, but we are primarily interested in spherical structures formed from asymmetric copolymers with long A blocks and short B blocks. The copolymer interface in a spherical micelle has a small radius of curvature; a typical spherical micelle has a radius (R) that is about $2-3$ times R_{gc}, the radius of gyration of the copolymer. The other extreme in curvature occurs when the copolymer is located at a flat interface, which is the situation when the AB copolymer molecules have just started to localize at the A−C interface (Figure 2c). In this case the radius of curvature is infinite. Intermediate values of the radius of curvature are achieved in the formation of swollen micelles. In swollen micelles, shown in Figure 2b, C homopolymer is solubilized in the center of an AB copolymer micelle. The radius of curvature for a swollen micelle can vary from near the radius of a micelle to much larger, depending on the strength of the interactions and the relative lengths of the molecules.

As the amount of A-rich copolymer at the interface increases, the preferred radius of curvature of the interface decreases from infinity to a lower, finite value. As the radius of curvature decreases further, swollen micelles can pinch off of at the A−C interface and move into the A matrix phase. If there are nanoparticles at the interface, they can also be encapsulated, as long as the copolymer interface retains its preferred radius of curvature. In this paper, we use self-consistent mean-field theory to calculate equilibrium volume fraction profiles for unswollen micelles, swollen micelles, and flat interfaces in this A, B, C three-component system to find equilibrium radii and determine the preferred state of the system.

Theoretical Formulation

The theoretical formulation begins with the free energy per unit volume for a homogeneous mixture of polymers, which can be written as[43,44]

$$\Delta f = \frac{k_B T}{\upsilon_0}\left\{\sum_k \frac{\phi_k \ln \phi_k}{N_k} + \frac{1}{2}\sum_{m\neq n}\chi_{mn}\phi_m\phi_n\right\} \tag{1}$$

where N_k and ϕ_k are the degrees of polymerization and volume fractions of each component k and χ_{mn} is the Flory interaction parameter between m and n repeat units. The volume fractions ϕ_m and ϕ_n refer to the total volume fraction of m and n repeat units. In our case, k can be *ha*, *hc*, or *cop* for A homopolymer, C homopolymer, or AB copolymer, respectively, and m can be *a*, *b*, or *c*, corresponding to A, B, or C repeat units. The subscripts *ca* and *cb* refer to the A and B blocks of the copolymer, respectively. The molecular volumes are normalized by a reference volume υ_0, and the interaction parameter is defined in terms of the same reference volume, typically the volume of one of the repeat units.

To find equilibrium volume fraction profiles that correspond to each of the structures we are interested in, we must know the chemical potential of each polymer. The chemical potential of each component, μ_k, is derived from the free energy expression and can be written as[43,44]

$$\frac{\mu_k}{k_B T} = \ln \phi_k + 1 - N_k\sum_k \frac{\phi_k}{N_k} + \frac{1}{k_B T}\sum_{j=1}^{N_k} w_p(j) \tag{2}$$

with

$$\frac{w_p(j)}{k_B T} = -\frac{1}{2}\sum_{m\neq n}\{\phi_m - \delta(m - p(j))\}\chi_{mn}\{\phi_n - \delta(n - p(j))\} \tag{3}$$

where j is an index that runs from unity at one end of the chain to N_k at the other end of the chain, and $p(j)$ is *a* if the jth repeat unit is A, *b* if the jth repeat unit is B, and *c* if the jth repeat unit is C. The delta functions are defined so that $\delta(m - p) = 1$ for $m = p$ and $\delta(m - p) = 0$ for $m \neq p$. The first three terms in the chemical potential are entropic terms arising from the interactions between each kind of polymer, while the last term accounts for the enthalpic interactions between each type of repeat unit. For a binary system with only A and B repeat units, eq 3 reduces to $w_a/k_B T = \chi_{ab}\phi_b^2$ and $w_b/k_B T = \chi_{ab}\phi_a^2$. The reference state for which $\mu_k = 0$ is a homopolymer melt with degree of polymerization N_k.

To generalize the theory for polymers of any composition distribution, we use the function $g_m(j)$, which is the average composition of m at repeat unit j along the backbone of a chain with N_k total repeat units.[45,46] The overall fraction of repeat unit m, f_m, is the average value of g_m:

$$f_m = \frac{1}{N_k}\sum_{j=1}^{N_k} g_m(j) \tag{4}$$

To account for this controlled composition distribution, the delta functions in w_p are replaced by the corresponding composition functions, g_m and g_n:

$$\frac{w_p(j)}{k_B T} = -\frac{1}{2}\sum_{m\neq n}\{\phi_m - g_m(j)\}\chi_{mn}\{\phi_n - g_n(j)\} \tag{5}$$

For a ternary system with A, B, and C repeat units, this becomes

$$\frac{w_p(j)}{k_B T} = -(\phi_a - g_a)\chi_{ab}(\phi_b - g_b) - (\phi_b - g_b)\chi_{bc}(\phi_c - g_c) - (\phi_a - g_a)\chi_{ac}(\phi_c - g_c) \quad (6)$$

The volume fractions ϕ_m and ϕ_n are obtained from the probability distribution functions $q_{k1}(\mathbf{r},j)$ and $q_{k2}(\mathbf{r},j)$, which are functions of the position $\mathbf{r}$ and the repeat unit j and start from opposite ends of the molecule. We consider systems with planar, cylindrical, or spherical symmetry, where the position $\mathbf{r}$ can be described in terms of a single discrete distance variable i.[44,47,48] The width of each layer i corresponds to a, the statistical segment length of one repeat unit. This length is defined such that R_{gc}, the unperturbed radius of gyration of a copolymer chain, is equal to $(N_{cop}/6a)^{1/2}$.

The two distribution functions describe possible configurations of the molecule on either side of a point located along the polymer chain backbone where the two functions meet. The volume fraction of repeat unit m in component k at a position i, $\phi_{km}(i)$, is given by summing over all possible junction points of q_{k1} and q_{k2}:

$$\phi_{km}(i) = \frac{1}{N_k}\exp(\mu_k/k_B T - 1)\sum_{j=1}^{N_k} q_{k1}(i,j)\, q_{k2}(i,N_k - j)\, g_m(j) \quad (7)$$

In this expression, the distribution functions are multiplied by $g_m(j)$ to account for the specific composition distribution of the molecule and are normalized by a factor that includes the chemical potential and degree of polymerization of the component.[21,44,45,49]

The distribution functions obey recursion relationships that arise from the connectivity of the chains:[44,47,48]

$$q_{k1}(i,j) = \{\lambda_{-1}q_{k1}(i-1,j-1) + \lambda_0 q_{k1}(i,j-1) + \lambda_{+1}q_{k1}(i+1,j-1)\}\exp\{-w(i,j)/k_B T\} \quad (8)$$

$$q_{k2}(i,j) = \{\lambda_{-1}q_{k2}(i-1,j-1) + \lambda_0 q_{k2}(i,j-1) + \lambda_{+1}q_{k2}(i+1,j-1)\}\exp\{-w(i,j)/k_B T\} \quad (9)$$

with the initial condition that $q_{k1}(i,0) = q_{k2}(i,0) = 1$. The transition probabilities λ_{-1}, λ_0, and λ_{+1} are the fractions of nearest-neighbor sites that lie in layer $i-1$, i, or $i+1$, respectively. For a simple cubic lattice, $\lambda_{-1} = \lambda_{+1} = 1/6$ and $\lambda_0 = 4/6$. The transition probabilities for systems with spherical or cylindrical symmetry are obtained by assuming that λ_{-1} and λ_{+1} are proportional to the contact areas between the layers, with λ_0 found by requiring the probabilities to sum to one:[50]

$$\lambda_{-1}(i) = \frac{1}{6}S(i-1)/L(i) \quad (10)$$

$$\lambda_{+1}(i) = \frac{1}{6}S(i)/L(i) \quad (11)$$

$$\lambda_0(i) = 1 - \lambda_{-1}(i) - \lambda_{+1}(i) \quad (12)$$

Here, $S(i)$ is the surface area between layers i and $i-1$ and $L(i)$ is the number of lattice sites within layer i. For a spherical geometry $S(i) = 4\pi i^2$, and for a cylindrical geometry $S(i) = 2\pi i l$, where l is the length of the cylinder. $L(i)$ is the difference in the total volumes V of systems with i and $i-1$ layers:

$$L(i) = V(i) - V(i-1) \quad (13)$$

For a spherical geometry, $V(i) = (4/3)\pi i^3$, and for a cylindrical geometry $V(i) = \pi i^2 l$.

Equations 8 and 9 are discrete representations of the modified diffusion equation introduced by Edwards[51] and used by many others:[49,52,53]

$$\frac{\partial q(r,n)}{\partial n} = \frac{a^2}{6}\left\{\frac{\partial^2 q(r,n)}{\partial r^2} + \frac{C}{r}\frac{\partial q(r,n)}{\partial r}\right\} - w(r,n)\, q(r,n) \quad (14)$$

where $C = 0$ for planar symmetry, $C = 1$ for cylindrical symmetry, and $C = 2$ for spherical symmetry. The variables r and n are the continuous forms of i and j.

The mean fields $w(r,n)$ or $w(i,j)$ are functions of both the local composition of the chain, $g(j)$, and the surrounding composition in the layer i, $\phi(i)$. The expression we use for $w(i,j)$ is based on the chemical potential and can be written as

$$w(i,j) = w_p(i,j) - k_B T\sum_k \frac{\phi_k(i)}{N_k} - \Delta w(i) + w_{ext}(i,j) \quad (15)$$

with

$$\frac{\Delta w(i)}{k_B T} = \zeta\{1 - \sum_k \phi_k(i)\} \quad (16)$$

The first term in the mean field expression, $w_p(i,j)$, is from the chemical potential and is the enthalpic contribution characterized by the χ parameters (eq 5). It is now a function of both i and j because the volume fractions are functions of i. The second term is the entropic contribution. The third term, $\Delta w(i)$, is associated with the incompressibility constraint, where ζ is inversely proportional to the bulk incompressibility of the system and is chosen to be high enough so that the results obtained are indistinguishable from the incompressible limit corresponding to $\zeta = \infty$.[21,44] The final term, $w_{ext}(i,j)$, accounts for any external fields acting on the system, such as the attractive interaction between the C homopolymer and the surface of a particle.

This set of mean-field equations is solved self-consistently for the volume fraction profiles of each component using boundary conditions corresponding to one of two cases. In the first case, there is a reflective boundary condition at $i = 0$, so that $q(0,j) = q(1,j)$. At the maximum i, i_{max}, there is a bulk phase boundary condition that assumes the matrix phase is homogeneous with $\Delta w(i_{max}) = 0$ and contains only A homopolymer and AB copolymer. This situation corresponds to an unswollen micelle (no C homopolymer) or a swollen micelle (C homopolymer in the center of the micelle) with planar, cylindrical, or spherical geometry (Figure 2a,b). In the second boundary condition case, there is a bulk phase boundary condition at both $i = 0$ and $i = i_{max}$. Again we assume homogeneous matrix phases with $\Delta w(i_{max}) = 0$ and $\Delta w(0) = 0$. We also assume that there is only A homopolymer and AB copolymer present at $i = i_{max}$ and only C homopolymer present at $i = 0$. Using planar symmetry, this corresponds to a flat interface between the two bulk phases of polymer (Figure 2c). In both cases, the equilibrium concentration profile is reached when the chemical potential of each component is uniform throughout the system.

The total free energy of the system can be written as follows:

$$F = \sum_k n_k \mu_k + F_{xs} \quad (17)$$

The first term is the contribution from the chemical potential

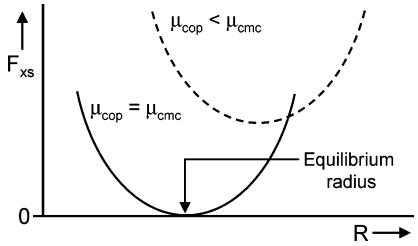

Figure 3. Schematic of the excess free energy associated with micelle formation, F_{xs}, as a function of R, the radius of the micelle. At the critical copolymer chemical potential, μ_{cmc}, $F_{xs} = 0$ at the equilibrium radius.

of each component, and the second term, F_{xs}, is the excess free energy in the system. This excess free energy is obtained by summing Δw over all of the lattice layers:

$$F_{xs} = \sum_i L(i)\,\Delta w(i) \tag{18}$$

In the case of a swollen or unswollen micelle, F_{xs} corresponds to the free energy associated with micelle formation, $\Delta F_{micelle}$. The critical copolymer chemical potential for the formation of micelles, μ_{cmc}, is the value at which $\Delta F_{micelle} = F_{xs} = 0$. To find μ_{cmc}, μ_{cop} is iterated until the solution gives $\Delta F_{micelle} = 0$ at the equilibrium radius, as shown schematically in Figure 3. In the case of a flat interface, F_{xs} corresponds to the interfacial free energy, or γ. The critical copolymer chemical potential, μ_γ, is the value where the interfacial energy vanishes, or $\gamma = 0$. The value of μ_γ is obtained in the same manner as μ_{cmc}, by iterating μ_{cop} to find the solution where $\gamma = F_{xs} = 0$.[44]

After finding the volume fraction profiles, we can also find the radii of the micelles. The radius of an unswollen spherical micelle, $R_{micelle}$, is found by using volume and surface area expressions and radially integrating the copolymer volume fraction, $\phi_{cop}(r)$, from zero to the maximum layer while subtracting the bulk value, $\phi_{cop}(\infty)$.

$$\frac{4}{3}\pi {R_{micelle}}^3 = \int_0^\infty (\phi_{cop}(r) - \phi_{cop}(\infty)) 4\pi r^2\,dr \tag{19}$$

The total radius of a swollen micelle, R_{tot}, is found in a similar manner by taking both ϕ_{cop} and ϕ_{hc} into account:

$$\frac{4}{3}\pi {R_{tot}}^3 = \int_0^\infty (\phi_{cop}(r) + \phi_{hc}(r) - \phi_{cop}(\infty) - \phi_{hc}(\infty)) 4\pi r^2\,dr \tag{20}$$

While formally defined by eqs 19 and 20, $R_{micelle}$ and R_{tot} also correspond to the radii at which the majority component changes from the A block of the copolymer to the A homopolymer. The radius of the C homopolymer in the center of the swollen micelle, R_{hc}, is written as

$$\frac{4}{3}\pi {R_{hc}}^3 = \int_0^\infty (\phi_{hc}(r) - \phi_{hc}(\infty)) 4\pi r^2\,dr \tag{21}$$

and also corresponds to the radius where the majority component changes from C homopolymer to the B block of the copolymer. The thickness of the copolymer in the radial direction, R_{cop}, is defined as the difference between R_{tot} and R_{hc}:

$$R_{cop} = R_{tot} - R_{hc} \tag{22}$$

All of the radii are in units of a, the width of one lattice layer, and are typically normalized by R_{gc}. Some other common parameters used when describing micelles can also be found

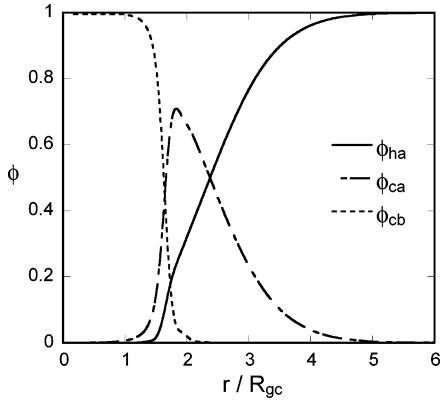

Figure 4. Radial volume fraction profile of an unswollen AB copolymer micelle (Figure 2a) in an A homopolymer matrix. $N_{ha} = N_{cop}$, $f_b = 0.2$, $\chi_{ab}N_{cop} = 60$, $\mu_{cmc}/k_BT = 5.38$, $R_{micelle}/R_{gc} = 2.63$.

from these radii. For example, the number of C homopolymer chains solubilized in a swollen micelle, Q^*_{hc}, is found from R_{hc} by dividing by the volume of a C homopolymer chain:

$$Q^*_{hc} = \frac{{}^4/_3\pi {R_{hc}}^3}{N_{hc}v_0} \tag{23}$$

Similarly, the interfacial excess of copolymer z^* is related to R_{cop}

$$z^* = {}^4/_3\pi {R_{tot}}^3 - {}^4/_3\pi {R_{hc}}^3 \tag{24}$$

and the number of copolymer molecules in a micelle, Q^*_{cop}, is

$$Q^*_{cop} = \frac{z^*}{N_{cop}v_0} \tag{25}$$

For a flat interface, Q^*_{cop} is the number of copolymer chains per area.

As shown in Figure 1, it may be possible to solubilize a solid spherical nanoparticle in the center of a swollen micelle by taking advantage of an attractive interaction between the particle and the C homopolymer, such as the attraction between PVP and gold. To incorporate the particle into the mean-field equations, the reflective boundary condition at $i = 0$ is replaced by a boundary condition corresponding to the surface of a solid particle. The polymer distribution functions are required to equal zero at $i = 0$ through $i = R_p$, the radius of the particle. To account for a preferential affinity of the C homopolymer for the solid surface, a term $w_{ext}(i)$ is applied to the C repeat units and set to a positive value at $i = R_p + 1$, with $w_{ext}(i) = 0$ for all other i and all other components.

Results and Discussion

Unswollen Micelles. A sample radial volume fraction profile for an unswollen spherical AB copolymer micelle in an A homopolymer matrix is shown in Figure 4, where r is the radial direction from the center of the micelle. For this calculation, $N_{ha} = N_{cop}$, $f_b = 0.2$, and $\chi_{ab}N_{cop} = 60$. These parameters are representative of a strongly segregated set of polymers where ϕ_{cmc} is still high enough for the system to equilibrate experimentally. This system forms spherical micelles, as shown by the micelle phase diagram calculated for $\chi_{ab}N_{cop} = 60$ in Figure 5. At each value of N_{ha}/N_{cop} and f_b in the phase diagram, the geometry with the lowest chemical potential of micelle formation, μ_{cmc}, is the equilibrium geometry. Regions favoring spherical, cylindrical, and lamellar micelles are shown. At very

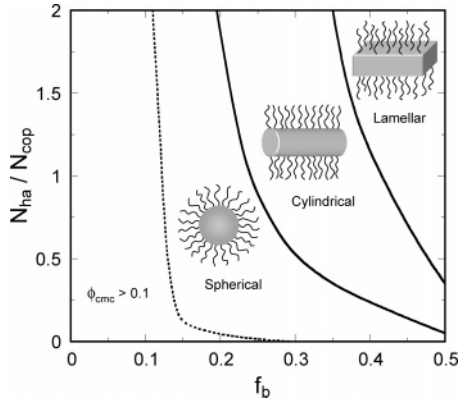

Figure 5. Micelle phase diagram at $\chi_{ab}N_{cop} = 60$ determined by the geometry with the lowest μ_{cmc}: spherical, cylindrical, or lamellar. N_{ha} and N_{cop} are the degrees of polymerization of the A homopolymer and AB diblock copolymer, respectively, and f_b is the fraction of B in the copolymer. In this paper we consider systems in the spherical region, with $N_{ha} = N_{cop}$ and $f_b = 0.2$.

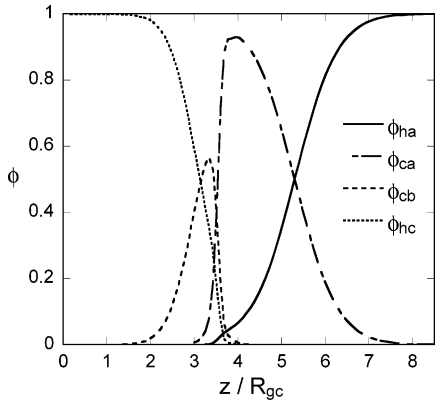

Figure 6. Volume fraction profile of an AB copolymer adsorbed at a flat interface (Figure 2c) between bulk A and C homopolymers. $N_{ha} = N_{cop}$, $N_{hc}/N_{cop} = 0.2$, $f_b = 0.2$, $\chi_{ab}N_{cop} = 60$, $\chi_{ac}N_{cop} = 60$, $\chi_{bc}N_{cb} = 0$, $\mu_\gamma/k_BT = 5.29$.

low values of f_b, the driving force for micellization is lessened, and the critical micelle concentration, ϕ_{cmc}, can be very high, or even non-existent. The region where ϕ_{cmc} is greater than 10% is also marked in Figure 5. The parameters we are interested in, $N_{ha}/N_{cop} = 1$ and $f_b = 0.2$, result in spherical micelles. These micelles form at $\mu_{cmc}/k_BT = 5.38$, which corresponds to a ϕ_{cmc} near 0.001, with an equilibrium radius of $R_{micelle}/R_{gc} = 2.63$, where R_{gc} is the radius of gyration of the copolymer, $(N_{cop}/6a)^{1/2}$.

Flat Interfaces. The copolymer interface in an unswollen micelle has a radius of curvature that is typically 2−3 times R_{gc}. The other extreme, an infinite radius of curvature, can be found when the copolymer segregates to a flat interface between two immiscible homopolymers. A sample volume fraction profile for an AB copolymer adsorbed at a flat interface between bulk A and C homopolymers is shown in Figure 6, where z is the direction normal to the interface and corresponds to the layer i. As before, this calculation uses the parameters $N_{ha} = N_{cop}$, $f_b = 0.2$, and $\chi_{ab}N_{cop} = 60$. In addition, there are three parameters associated with the C homopolymer: $N_{hc}/N_{cop} = 0.2$, $\chi_{ac}N_{cop} = 60$, and $\chi_{bc}N_{cb} = 0$. The interaction parameter χ_{ac} is set equal to χ_{ab} in all cases. In this particular example, $\chi_{bc}N_{cb}$ is set equal to zero, representing the case where the C homopolymer acts as a B homopolymer. These parameters give $\mu_\gamma/k_BT = 5.29$, where we define μ_γ as the copolymer chemical potential where the interfacial tension for a flat interface reaches zero.

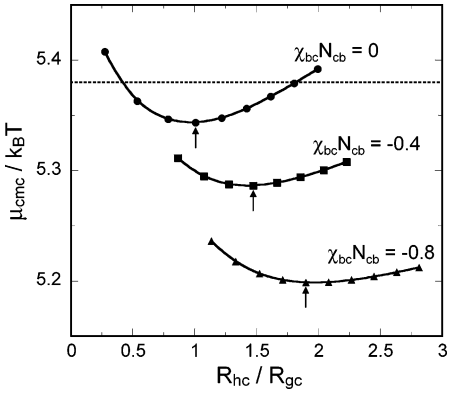

Figure 7. Chemical potential of swollen micelle formation (μ_{cmc}) as a function of R_{hc}/R_{gc} with varying χ_{bc}. The chemical potential of unswollen micelle formation is indicated by the dotted line (- - -). $N_{hc}/N_{cop} = 0.75$, $N_{ha} = N_{cop}$, $f_b = 0.2$, $\chi_{ab}N_{cop} = 60$, $\chi_{ac}N_{cop} = 60$.

Swollen Micelles. An intermediate copolymer interfacial radius of curvature is achieved in the case of a swollen micelle, where C homopolymer is solubilized in the center of a spherical AB copolymer micelle. While the radius of an unswollen micelle is determined by the copolymer length, which is fixed, the radius of a swollen micelle is determined by the amount of C homopolymer that is solubilized in the center. Because this amount is easily varied, there are many self-consistent solutions that all have $F_{xs} = 0$. There are two contributions to the free energy in eq 17: the contribution from the chemical potential and F_{xs}. If $F_{xs} = 0$, the total free energy will be minimized by minimizing μ_{cmc}, assuming a constant number of molecules. Thus, the equilibrium solution is the one with the lowest μ_{cmc}. Figure 7 shows all of the solutions for $N_{hc}/N_{cop} = 0.75$ at three different values of $\chi_{bc}N_{cb}$. The solutions occur at discrete intervals in r due to the discretization method used to solve the mean-field equations. The minimum in each curve is indicated by an arrow and represents the solution with the equilibrium amount of C homopolymer in the center of the micelle. The values of μ_{cmc} and R_{hc} associated with this solution are the equilibrium values of the chemical potential and radius. The volume fraction profiles for all three minima are shown in Figure 8. As the value of $\chi_{bc}N_{cb}$ is lowered from 0 to −0.4 and −0.8, representing an increasing attraction between B and C repeat units, the equilibrium μ_{cmc} is also lowered, indicating that the swollen micelles become easier to form. Also, the equilibrium R_{hc} increases with decreasing $\chi_{bc}N_{cb}$, indicating that an increasing attraction causes more C homopolymer to be solubilized in the micelle. Borukhov and Leibler[54,55] use theory and Brown et al.[56] use experiments to show that in the case of a polymer brush immersed in a polymer melt an attractive enthalpic interaction (negative χ) can change the conformation of the brush polymer from a dry to a wet brush. In the wet brush, the polymer is extended, and the degree to which the two polymers mix increases. In our study, the B block of the copolymer can be thought of as a brush extending from the interface where the A−B copolymer junction points are localized. With increasingly negative χ_{bc}, a higher fraction of C homopolymer mixes with the B block, which changes the volume fraction profile ϕ_{cb}, as seen in Figure 8. All of the equilibrium values of μ_{cmc} for the swollen micelles are below the chemical potential of unswollen micelle formation, which is indicated by the dotted line in Figure 7. At this value of N_{hc}/N_{cop}, swollen micelles will form before micellization would occur in the absence of C homopolymer.

A sample radial volume fraction profile for an equilibrium swollen micelle with the same parameters used in Figures 5 and 6 is shown in Figure 9. In this case, when N_{hc}/N_{cop} is low,

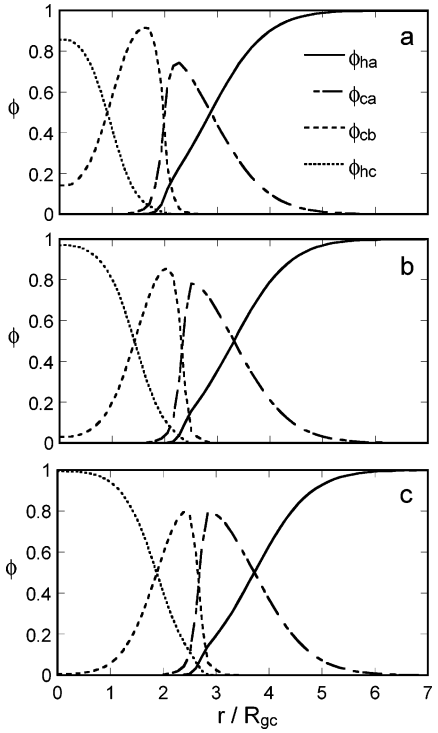

Figure 8. Volume fraction profiles of C homopolymer-swollen AB copolymer micelles in an A homopolymer matrix corresponding to the minima in Figure 7. $N_{ha} = N_{cop}$, $N_{hc}/N_{cop} = 0.75$, $f_b = 0.2$, $\chi_{ab}N_{cop} = 60$, $\chi_{ac}N_{cop} = 60$. (a) $\chi_{bc}N_{cb} = 0$, (b) $\chi_{bc}N_{cb} = -0.4$, (c) $\chi_{bc}N_{cb} = -0.8$.

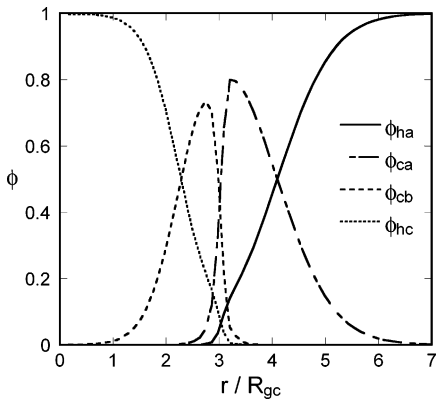

Figure 9. Volume fraction profile of an AB copolymer micelle in an A homopolymer matrix with C homopolymer solubilized in the center (Figure 2b). $N_{ha} = N_{cop}$, $N_{hc}/N_{cop} = 0.2$, $f_b = 0.2$, $\chi_{ab}N_{cop} = 60$, $\chi_{ac}N_{cop} = 60$, $\chi_{bc}N_{cb} = 0$, $\mu_{cmc}/k_BT = 5.02$, $R_{tot}/R_{gc} = 4.21$.

even with $\chi_{bc} = 0$ there is a pure C homopolymer phase in the center of the micelle. This swollen micelle forms at $\mu_{cmc}/k_BT = 5.02$ and has a radius of $R_{tot}/R_{gc} = 4.21$. The three examples in Figures 5, 6, and 9 demonstrate that for $N_{hc}/N_{cop} = 0.2$ and $\chi_{bc}N_{cb} = 0$ the swollen micelle has the lowest chemical potential of formation, meaning that the swollen micelle will form before the interfacial tension of a flat interface reaches zero and before bulk micellization occurs.

These results are summarized in Figure 10 in a plot of the three critical chemical potentials as functions of N_{hc}/N_{cop} for two different values of $\chi_{bc}N_{cb}$. At all values of N_{hc}/N_{cop}, μ_γ is greater than μ_{cmc} for both swollen and unswollen micelles. For $\chi_{bc}N_{cb} = 0$ and at low values of N_{hc}/N_{cop}, μ_{cmc} is lower for swollen micelles than for unswollen micelles. At a slightly negative χ_{bc}, $\chi_{bc}N_{cb} = -0.4$, swollen micelles always have the lowest chemical potential of formation.

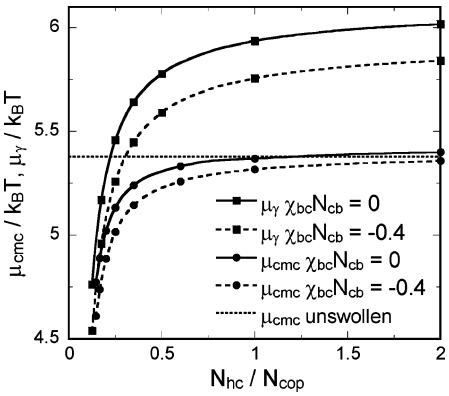

Figure 10. Critical copolymer chemical potential (μ_{cmc} for unswollen and swollen micelles, μ_γ for flat interface) as a function of N_{hc}/N_{cop} for $\chi_{bc} = 0$ and $\chi_{bc} < 0$. $N_{ha} = N_{cop}$, $f_b = 0.2$, $\chi_{ab}N_{cop} = 60$, $\chi_{ac}N_{cop} = 60$.

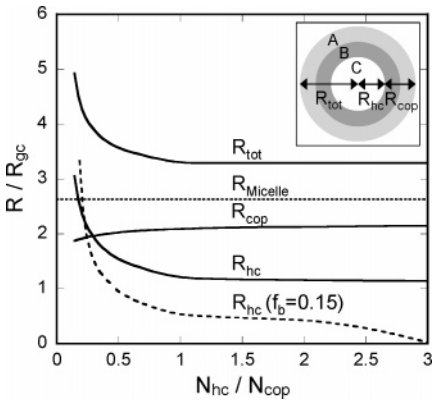

Figure 11. Swollen and unswollen radii as defined in eqs 19−22 as functions of N_{hc}/N_{cop} for $N_{ha} = N_{cop}$, $f_b = 0.2$, $\chi_{ab}N_{cop} = 60$, $\chi_{ac}N_{cop} = 60$, and $\chi_{bc}N_{cb} = 0$. R_{hc} is also shown for $f_b = 0.15$.

The radius of the swollen micelle also varies with N_{hc}/N_{cop}, as shown in Figure 11. In this figure, R_{tot}, R_{cop}, and R_{hc} are plotted for a swollen micelle with the same parameters as in Figure 9 but with varying N_{hc}/N_{cop}. The total swollen micelle radius, R_{tot}, is determined by the radius of the C homopolymer core, R_{hc}. The copolymer has a preferred length, so R_{cop} remains nearly constant over a wide range of N_{hc}/N_{cop}. The plot also shows that R_{hc} decreases with increasing N_{hc}/N_{cop}. As the length of the C homopolymer chains increases, confinement effects cause solubilization of the homopolymer to be less favorable, so the radius decreases as less homopolymer is included in the micelle. In addition to the data for $f_b = 0.2$, R_{hc} is also plotted for a copolymer with $f_b = 0.15$. With a shorter B block, the copolymer micelle is no longer able to support long C homopolymer chains in the core, so R_{hc} decreases to zero at large values of N_{hc}/N_{cop}. In this case, though it is not shown in the figure, R_{cop} approaches $R_{micelle}$, and when there is no longer C homopolymer in the core, the swollen micelle becomes an unswollen micelle.

Nanocomposite. A nanoparticle can be included in the center of a swollen micelle by including an external field term, w_{ext}-(i), in the expression for the mean field. This term creates a favorable interaction between the surface of the particle and the C repeat units and forces a layer of C homopolymer to form around the particle. Volume fraction profiles for three nanoparticle radii are shown in Figure 12. In Figure 12a there is no nanoparticle, and the volume fraction profile is the same as the one in Figure 9. In Figure 12b, all of the parameters are the same except there is a particle in the center with radius $R_p/R_{gc} = 0.7$. In this case, the particle is smaller than the region of

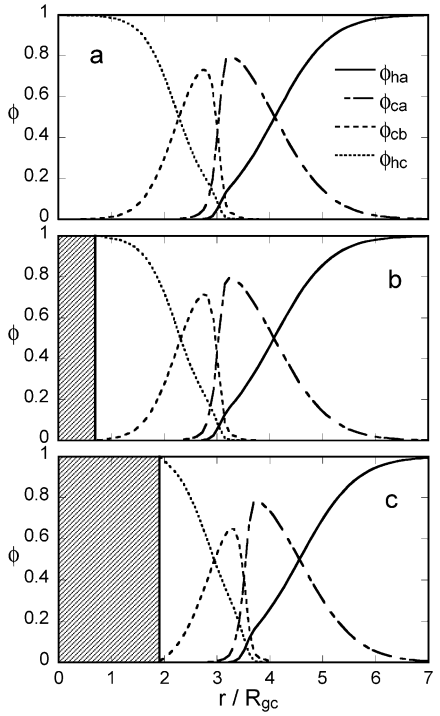

Figure 12. Volume fraction profiles for swollen micelles with particles of various size in the center: (a) $R_p/R_{gc} = 0$, (b) $R_p/R_{gc} = 0.7$, (c) $R_p/R_{gc} = 1.9$. $N_{hc}/N_{cop} = 0.2$, $N_{ha} = N_{cop}$, $f_b = 0.2$, $\chi_{ab}N_{cop} = 60$, $\chi_{ac}N_{cop} = 60$, $\chi_{bc}N_{cb} = 0$.

pure C homopolymer in the core, and the particle has no effect on the volume fraction profile. In Figure 12c, the particle radius is $R_p/R_{gc} = 1.9$, which is larger than the core of pure C homopolymer. In this case, there is still a thin layer of C homopolymer surrounding the particle, and the concentration profiles of all the other components are shifted outward.

Conclusions

We have investigated an A, B, C three-component system that consists of A homopolymer, AB copolymer, and C homopolymer, where there are attractive interactions between the B and C components. This system represents many possible experimental systems; one example is a system where A is polystyrene, B is poly(4-hydroxystyrene), and C is poly(2-vinylpyridine). We use self-consistent mean-field theory to calculate volume fraction profiles for unswollen and swollen micelles as well as flat interfaces using a theory that is generalized for multiple components and a general copolymer composition distribution. We calculate the swollen and unswollen micelle chemical potentials of formation and radii and compare them. We also compare the micelles to the case of a flat interface, to determine which of these three structures occurs in equilibrium.

There is a wide set of conditions that could be investigated in this system, but we chose to focus on strongly segregating A−B and A−C pairs with $\chi_{ab}N_{cop} = \chi_{ac}N_{cop} = 60$ and a copolymer composition of $f_b = 0.2$, which lies in the spherical region of the micelle phase diagram. The A homopolymer and AB copolymer lengths are always equal, but we vary the length of the C homopolymer. We also vary the interaction parameter χ_{bc} from 0 to slightly negative values to simulate an attractive interaction between the B and C repeat units.

The important parameter governing the formation of swollen spherical micelles is the radius of curvature of the copolymer interface. As copolymer accumulates at the A−C interface, the preferred radius of curvature changes from infinite to a lower value, and swollen micelles can pinch off and move into the A matrix phase. The swollen micelles have a preferred radius that controls the amount of C homopolymer solubilized in the center of the micelles. When χ_{bc} is negative, the copolymer chemical potential in swollen micelles is always lower than the copolymer chemical potential in unswollen micelles, and micellization is promoted by the presence of C homopolymer. The copolymer chemical potential required for micelle formation (μ_{cmc}) can also be compared to the copolymer chemical potential where the interfacial tension of a flat interface reaches zero (μ_γ). In the region of the micelle phase diagrams where the equilibrium micelles are spherical, curved interfaces are favored and μ_{cmc} is less than μ_γ.

Mean-field calculations also show that nanoparticles can be encapsulated in the center of swollen micelles by including an external field term that creates an attraction between the surface of the particle and the C homopolymer, such as the attraction between PVP and gold. If the nanoparticle radius is smaller than the equilibrium radius of C homopolymer at the same conditions without a particle, there is no change in the concentration profile when the particle is incorporated into the swollen micelle. If the radius of the particle is larger than the equilibrium radius of C homopolymer, a thin layer of C homopolymer forms at the surface of the particle and the other concentration profiles are shifted outward. These results indicate that a nanocomposite could be formed by utilizing the attractive B−C interactions to encapsulate particles and C homopolymer in AB diblock copolymer micelles.

Acknowledgment. This work was supported by the MRSEC program of the National Science Foundation (DMR-0076097) at the Materials Research Center of Northwestern University, and by a NSF Graduate Research Fellowship.

References and Notes

(1) Segalman, R. A. *Mater. Sci. Eng. R* **2005**, *48*, 191.
(2) Park, C.; Yoon, J.; Thomas, E. L. *Polymer* **2003**, *44*, 6725.
(3) Fasolka, M. J.; Mayes, A. M. *Annu. Rev. Mater. Res.* **2001**, *31*, 323.
(4) Xiang, H. Q.; Lin, Y.; Russell, T. P. *Macromolecules* **2004**, *37*, 5358.
(5) Green, P. F.; Limary, R. *Adv. Colloid Interface Sci.* **2001**, *94*, 53.
(6) Park, M.; Harrison, C.; Chaikin, P. M.; Register, R. A.; Adamson, D. H. *Science* **1997**, *276*, 1401.
(7) Chiu, J. J.; Kim, B. J.; Kramer, E. J.; Pine, D. J. *J. Am. Chem. Soc.* **2005**, *127*, 5036.
(8) Lee, J. Y.; Thompson, R. B.; Jasnow, D.; Balazs, A. C. *Phys. Rev. Lett.* **2002**, *89*.
(9) Lee, J. Y.; Thompson, R. B.; Jasnow, D.; Balazs, A. C. *Macromolecules* **2002**, *35*, 4855.
(10) Lee, J. Y.; Thompson, R. B.; Jasnow, D.; Balazs, A. C. *Faraday Discuss.* **2003**, *123*, 121.
(11) Lee, J. Y.; Balazs, A. C.; Thompson, R. B.; Hill, R. M. *Macromolecules* **2004**, *37*, 3536.
(12) Lin, Y.; Boker, A.; He, J. B.; Sill, K.; Xiang, H. Q.; Abetz, C.; Li, X. F.; Wang, J.; Emrick, T.; Long, S.; Wang, Q.; Balazs, A.; Russell, T. P. *Nature (London)* **2005**, *434*, 55.
(13) Thompson, R. B.; Ginzburg, V. V.; Matsen, M. W.; Balazs, A. C. *Science* **2001**, *292*, 2469.
(14) Thompson, R. B.; Lee, J. Y.; Jasnow, D.; Balazs, A. C. *Phys. Rev. E* **2002**, *66*.
(15) Thompson, R. B.; Ginzburg, V. V.; Matsen, M. W.; Balazs, A. C. *Macromolecules* **2002**, *35*, 1060.
(16) Chervanyov, A. I.; Balazs, A. C. *J. Chem. Phys.* **2003**, *119*, 3529.
(17) Ginzburg, V. V.; Qiu, F.; Balazs, A. C. *Polymer* **2001**, *43*, 461.
(18) Zhang, C. L.; Xu, T.; Butterfield, D.; Misner, M. J.; Ryu, D. Y.; Emrick, T.; Russell, T. P. *Nano Lett.* **2005**, *5*, 357.
(19) Shi, Z. T.; Han, M.; Zhao, S. F.; Zhang, L.; Li, X. F.; Wan, H. G.; Wang, G. H. *Int. J. Mod. Phys. B* **2005**, *19*, 2792.
(20) Lopes, W. A.; Jaeger, H. M. *Nature (London)* **2001**, *414*, 735.
(21) Shull, K. R.; Kramer, E. J. *Macromolecules* **1990**, *23*, 4769.
(22) Shull, K. R.; Kramer, E. J.; Hadziioannou, G.; Tang, W. *Macromolecules* **1990**, *23*, 4780.

(23) Shull, K. R.; Kellock, A. J.; Deline, V. R.; Macdonald, S. A. *J. Chem. Phys.* **1992**, *97*, 2095.
(24) Hu, W. C.; Koberstein, J. T.; Lingelser, J. P.; Gallot, Y. *Macromolecules* **1995**, *28*, 5209.
(25) Reynolds, B. J.; Ruegg, M. L.; Mates, T. E.; Radke, C. J.; Balsara, N. P. *Macromolecules* **2005**, *38*, 3872.
(26) Liang, H.; Favis, B. D.; Yu, Y. S.; Eisenberg, A. *Macromolecules* **1999**, *32*, 1637.
(27) Gersappe, D.; Balazs, A. C. *Phys. Rev. E* **1995**, *52*, 5061.
(28) Lyatskaya, Y.; Gersappe, D.; Gross, N. A.; Balazs, A. C. *J. Phys. Chem.* **1996**, *100*, 1449.
(29) Lyu, S.; Jones, T. D.; Bates, F. S.; Macosko, C. W. *Macromolecules* **2002**, *35*, 7845.
(30) Shi, T. F.; Ziegler, V. E.; Welge, I. C.; An, L. J.; Wolf, B. A. *Macromolecules* **2004**, *37*, 1591.
(31) Sundararaj, U.; Macosko, C. W. *Macromolecules* **1995**, *28*, 2647.
(32) Anastasiadis, S. H.; Gancarz, I.; Koberstein, J. T. *Macromolecules* **1989**, *22*, 1449.
(33) Bucknall, D. G.; Higgins, J. S.; Rostami, S. *Polymer* **1992**, *33*, 4419.
(34) Xu, Z. H.; Kramer, E. J.; Edgecombe, B. D.; Frechet, J. M. J. *Macromolecules* **1997**, *30*, 7958.
(35) Edgecombe, B. D.; Frechet, J. M. J.; Xu, Z. H.; Kramer, E. J. *Chem. Mater.* **1998**, *10*, 994.
(36) Edgecombe, B. D.; Stein, J. A.; Frechet, J. M. J.; Xu, Z. H.; Kramer, E. J. *Macromolecules* **1998**, *31*, 1292.
(37) Dai, K. H.; Kramer, E. J.; Frechet, J. M. J.; Wilson, P. G.; Moore, R. S.; Long, T. E. *Macromolecules* **1994**, *27*, 5187.
(38) Matsen, M. W. *J. Chem. Phys.* **1999**, *110*, 4658.
(39) Xu, Z.; Jandt, K. D.; Kramer, E. J.; Edgecombe, B. D.; Frechet, J. M. J. *J. Polym. Sci., Part B: Polym. Phys.* **1995**, *33*, 2351.
(40) Jiao, J. B.; Kramer, E. J.; de Vos, S.; Moller, M.; Koning, C. *Polymer* **1999**, *40*, 3585.
(41) Israels, R.; Jasnow, D.; Balazs, A. C.; Guo, L.; Krausch, G.; Sokolov, J.; Rafailovich, M. *J. Chem. Phys.* **1995**, *102*, 8149.
(42) Dan, N.; Safran, S. A. *Macromolecules* **1994**, *27*, 5766.
(43) Evers, O. A.; Scheutjens, J.; Fleer, G. J. *Macromolecules* **1990**, *23*, 5221.
(44) Shull, K. R. *Macromolecules* **1993**, *26*, 2346.
(45) Shull, K. R. *Macromolecules* **2002**, *35*, 8631.
(46) Lefebvre, M. D.; Olvera de la Cruz, M.; Shull, K. R. *Macromolecules* **2004**, *37*, 1118.
(47) Scheutjens, J.; Fleer, G. J. *J. Phys. Chem.* **1979**, *83*, 1619.
(48) Scheutjens, J.; Fleer, G. J. *J. Phys. Chem.* **1980**, *84*, 178.
(49) Hong, K. M.; Noolandi, J. *Macromolecules* **1981**, *14*, 727.
(50) Leermakers, F. A. M.; Scheutjens, J. M. H. M. *J. Phys. Chem.* **1989**, *93*, 7417.
(51) Edwards, S. F. *Proc. Phys. Soc., London* **1965**, *85*, 613.
(52) Helfand, E.; Wasserman, Z. R. *Macromolecules* **1976**, *9*, 879.
(53) Helfand, E. *Macromolecules* **1975**, *8*, 552.
(54) Borukhov, I.; Leibler, L. *Macromolecules* **2002**, *35*, 5171.
(55) Borukhov, I.; Leibler, L. *Phys. Rev. E* **2000**, *62*, R41.
(56) Brown, H. R.; Char, K.; Deline, V. R. *Macromolecules* **1990**, *23*, 3383.

MA060112W